JOURNAL OF Materials CHEMISTRY

# Synthesis of new vanadium–chromium and chromium–molybdenum oxynitrides by direct ammonolysis of freeze-dried precursors

**Abdelouahad El-Himri, Fernando Sapiña,* Rafael Ibañez and Aurelio Beltrán**

*Institut de Ciència dels Materials de la Universitat de València, Apartado de Correos 2085, E-46071 València, Spain. E-mail: fernando.sapina@uv.es*

***Received 1st June 2000, Accepted 31st July 2000***
***First published as an Advance Article on the web 22nd September 2000***

Interstitial vanadium–chromium and chromium–molybdenum oxynitrides in the solid solution series $V_{1-z}Cr_z(O_xN_y)$ and $Cr_{1-z}Mo_z(O_xN_y)$ ($z=0.0$, 0.2, 0.4, 0.5, 0.6, 0.8, 1.0) have been obtained by direct ammonolysis of precursors resulting from the freeze-drying of aqueous solutions of the appropriate metal salts. A study of the influence of the preparative variables on the outcomes of this procedure is presented. Compounds in the $V_{1-z}Cr_z(O_xN_y)$ series are prepared as single phases by nitridation at 1073 K, followed by fast cooling of the samples. Compounds in the $Cr_{1-z}Mo_z(O_xN_y)$ series are prepared as nearly single phases by nitridation at different temperatures, optimized for each composition, followed by fast cooling of the samples. As for the VN, CrN and $Mo_2N$ binary nitrides, all the $V_{1-z}Cr_z(O_xN_y)$ and $Cr_{1-z}Mo_z(O_xN_y)$ compounds in these series have the rock salt crystal structure, in which the metal atoms are in a fcc arrangement, with non-metal atoms occupying octahedral interstitial positions. The materials have been characterized by X-ray powder diffraction, elemental analysis, scanning electron microscopy and thermogravimetry under oxygen flow. $V_{1-z}Cr_z(O_xN_y)$ and $Cr_{1-z}Mo_z(O_xN_y)$ grains are aggregates of nanometric spherical particles with diameters typically around 20 nm. Surface oxidation must account to a large extent for the oxygen content of these compounds.

## Introduction

In a recent publication concerning the chemistry of vanadium–molybdenum oxynitrides,[1] we referred to catalysis as one of the emerging fields of application that are currently leading to a renewal in interest in transition metal carbides and nitrides.[2] In that work, we showed how the known catalyst $V_2Mo(O_xN_y)$, which has attracted considerable attention due to its exceptional catalytic activity in processes involving hydrogen transfer reactions,[3] represents only one point in the $V_{1-z}Mo_z(O_xN_y)$ ($0\leqslant z\leqslant 1$) solid solution series.[1] We then concluded that, as far as the catalytic activity in the V–Mo–O–N system must depend on the stoichiometric metal ratio, it should be possible to assay different compositions in this system to optimize the catalytic properties. Our success with this system was based on the development of a new processing route involving the use of precursors resulting from freeze-drying of aqueous solutions of common metal salts.[4] Besides overcoming the problem of variable metal stoichiometry[4,5] along the entire bimetallic $V_{1-z}Mo_z(O_xN_y)$ ($0\leqslant z\leqslant 1$) solid solution series, this alternative solution-based synthetic procedure might be especially suitable for the preparation of supported catalysts.

In the present work, we report on how the use of freeze-dried bimetallic precursors has also allowed us to prepare oxynitrides in two new solid solution series closely related to that above, $V_{1-z}Cr_z(O_xN_y)$ and $Cr_{1-z}Mo_z(O_xN_y)$ ($0\leqslant z\leqslant 1$). The consequent compositional variability suggests new possibilities for the optimization of the catalytic properties of the V–Mo–O–N materials.

## Experimental

### Synthesis

Materials used as reagents in the current investigation were $NH_4VO_3$ (Fluka, 99.0%), $(NH_4)_2CrO_4$ (Panreac, 99.5%) and $(NH_4)_6Mo_7O_{24}\cdot 4H_2O$ (Panreac, 99.0%). Initial V, Cr or Mo-containing solutions were prepared by dissolving their respective salts in distilled water. These were combined to obtain V–Cr and Cr–Mo source solutions with total cationic concentrations of 0.50 M, and nominal molar compositions V : Cr or Cr : Mo = $1-z:z$ ($z=0.00$, 0.20, 0.40, 0.50, 0.60, 0.80, 1.00). The masses of the different reagents were adjusted to give 5 g of the final products. Droplets of these solutions were flash frozen by projection on liquid nitrogen and then freeze-dried at a pressure of 1–10 Pa in a Telstar Cryodos freeze-drier. In this way, dried solid precursors were obtained as amorphous (by X-ray diffraction) loose powders.

V–Cr and Cr–Mo oxynitrides were synthesized by ammonolysis of the amorphous precursor solids (Tables 1 and 2). The gases employed were $NH_3$ (99.9%) and $N_2$ (99.9995%). A sample of the selected precursor (*ca.* 0.5 g) was placed into an alumina boat, which was then inserted into a quartz flow-through tube furnace. The back end of the tube furnace was connected to an acetic acid trap and the front end was connected to the gas line. Prior to initiating the thermal treatment, the tube furnace was purged for 30 min with $N_2$ and another 30 min with $NH_3$. Several runs under different experimental conditions were also performed in order to determine the appropriate conditions for the preparation of pure samples. The precursor powder was heated at 5 K min$^{-1}$ to a final temperature ($T_f$) that was held for a period of time ($t_{hold}$) under flowing ammonia (50 cm$^3$ min$^{-1}$). Then, the solid was cooled down at different variable rates ($r_c$) under the same atmosphere. The different cooling rates were obtained by either turning off the oven and leaving the sample inside (slow, *ca.* 2 K min$^{-1}$) or by quenching at room temperature (fast, *ca.* 50 K min$^{-1}$). After cooling, the product was passivated with $N_2$ for 30 min.

From these experiments, it was found that single phase samples in the V–Cr–O–N system are obtained at 1073 K, independent of the cooling rate (fast or slow). Nevertheless, insofar as it was previously found that the preparation of the closely related V–Mo–O–N samples required the use of a fast

DOI: 10.1039/b004400h

**Table 1** Chemical composition, cell parameter and crystallite size of vanadium–chromium oxynitrides $V_{1-z}Cr_z(O_xN_y)$

| $z$ | $z$ (EDAX)[a] | Oxygen (wt%) | Nitrogen (wt%) | Proposed stoichiometry | Cell parameter, $a$/Å | $t$/nm |
|---|---|---|---|---|---|---|
| 0.0 | — | 3.1(3) | 19.8(6) | $V(O_{0.13}N_{0.93})$ | 4.13161(9) | 37 |
| 0.2 | 0.20 | 2.0(2) | 22.1(7) | $V_{0.8}Cr_{0.2}(O_{0.08}N_{1.06})$ | 4.13423(20) | 41 |
| 0.4 | 0.40 | 1.1(1) | 21.4(6) | $V_{0.6}Cr_{0.4}(O_{0.05}N_{1.01})$ | 4.13603(10) | 37 |
| 0.5 | 0.51 | 3.8(3) | 18.7(6) | $V_{0.5}Cr_{0.5}(O_{0.16}N_{0.89})$ | 4.13698(9) | 38 |
| 0.6 | 0.60 | 2.8(2) | 20.3(6) | $V_{0.4}Cr_{0.6}(O_{0.12}N_{0.97})$ | 4.13768(12) | 33 |
| 0.8 | 0.79 | 2.8(2) | 19.4(6) | $V_{0.2}Cr_{0.8}(O_{0.12}N_{0.92})$ | 4.14177(9) | 34 |
| 1.0 | — | 3.5(3) | 15.9(5) | $Cr(O_{0.14}N_{0.67})$ | 4.14439(9) | 34 |

[a]Estimated absolute error in $z$ is 0.02.

cooling rate,[1] we have also systematically prepared V and Cr-containing samples using a fast cooling rate. Thus, for the preparation of pure samples, the precursor powder was heated at 5 K $min^{-1}$ under flowing ammonia (50 $cm^3$ $min^{-1}$) to a final temperature of 1073 K. The samples were held at the reaction temperature for 2 h and then quenched to room temperature. After cooling, the resulting solid was purged with $N_2$ for 30 min. All products were stored in a desiccator over $CaCl_2$.

Concerning the Cr–Mo–O–N system, treatments similar to that above resulted in the presence of impurities (chromium and molybdenum oxides). Therefore, we carried out thermal treatments for longer times (12 h) and the nitridation temperature was optimized for each composition (Table 2) in order to minimize the amount of impurities. After quenching to room temperature, the resulting solids were purged with $N_2$ for 30 min. All products were stored in a desiccator over $CaCl_2$.

### Characterization

**Elemental analysis.** Metal ratios in the solids were determined by energy dispersive X-ray analysis (EDAX) on a Jeol JSM 6300 scanning electron microscope using an Oxford detector with quantification performed using virtual standards on associated Link-Isis software. The operating voltage was 20 kV and the energy range of the analysis 0–20 keV. The nitrogen content of the oxynitrides was evaluated by standard combustion analysis (LECO CHNS-932); $N_2$ and CO were separated in a chromatographic column, and measured using a thermal conductivity detector. The oxygen content was indirectly determined by thermogravimetric analysis (Perkin Elmer TGA 7 system). The results of these analyses for the resulting oxynitrides are summarized in Tables 1 and 2.

**X-Ray diffraction.** X-Ray powder diffraction patterns were obtained from a Siemens D501 automated diffractometer using graphite-monochromated Cu-K$\alpha$ radiation. Samples were dusted through a sieve on the holder surface. Routine patterns for phase identification were collected with a scanning step of 0.08° in 2$\theta$ over the angular range 2$\theta$ 30–70° with a collection time of 5 s per step. The cell parameters of each product were obtained by profile fitting of the pattern using the Le Bail method,[6] as implemented in the FULLPROF program,[7] from patterns collected with a scanning step of 0.02° in 2$\theta$ over a wider angular range (2$\theta$ 30–90°) and with a longer acquisition time (10 s per step) in order to enhance statistics. The fits were performed using a pseudo-Voigt peak-shape function. In the final runs, the usual profile parameters (scale factors, background coefficients, zero-points, half-widths, pseudo-Voigt and asymmetry parameters for the peak shape) were refined. All graphical representations relating to X-ray powder diffraction patterns were performed using the DRXWin Program.[8]

**Microstructural characterization.** The morphology of both the crystalline precursors and the resulting oxynitrides was observed using a scanning electron microscope (Hitachi S-4100) operating at an accelerating voltage of 30 kV. All the preparations were covered with a thin film of gold for better image definition.

## Results and discussion

It is well known that two isostructural transition metal nitrides may form a bimetallic solid solution provided that their lattice parameters differ by no more than about 10–15%. Rock salt-type interstitial (with N atoms occupying octahedral sites) crystalline phases, which are tolerant to a certain non-stoichiometry range, have been characterized in each one of the individual V–N, Cr–N and Mo–N systems. Indeed, the respective compositions for the cubic nitride phases have been established as $\delta$-$VN_{1-x}$ ($0 \leqslant x \leqslant 0.15$–$0.20$), $\delta$-$CrN_{1-x}$ (with a narrow range of $x$ values) and $\gamma$-$Mo_2N_{1+x}$ ($-0.2 \leqslant x \leqslant 0.3$).[9] According to the JCPDS database, the cell parameter of the cubic structure (stoichiometric compositions) varies from 4.139 (V) to 4.140 (Cr) and 4.163 Å (Mo). With such limit values (they differ by less than 1%), there should be no problem *a priori* to form cubic nitride solid solutions involving any pair of metals among the three mentioned (V, Cr and Mo). However, the rock salt phases are not the only phases that can be prepared in the parent nitride systems.[9] The multiphasic character of these systems implies, therefore, a clear synthetic limitation in order to obtain polymetallic rock salt-type nitride solid solutions.

As mentioned in the Introduction, we recently reported on the existence of the solid solution $V_{1-z}Mo_z(O_xN_y)$ ($0 \leqslant z \leqslant 1$), based on a fcc array of metal atoms.[1] We then showed that, under our synthetic approach, the experimental conditions appropriate to the preparation of rock salt-type single phase samples of the nitride containing Mo only are significantly more restrictive (973–1073 K; quenching is required) than in the case of the nitride containing V only (773–1173 K; independent of the cooling rate). Thus, our first goal in this

**Table 2** Chemical composition, cell parameter and crystallite size of chromium–molybdenum oxynitrides $Cr_{1-z}Mo_z(O_xN_y)$

| $z$ | $T_f$/K | $z$ (EDAX)[a] | Oxygen (wt%) | Nitrogen (wt%) | Proposed stoichiometry | Cell parameter, $a$/Å | $t$/nm |
|---|---|---|---|---|---|---|---|
| 0.0 | 1023 | — | 1.5(1) | 20.8(6) | $Cr(O_{0.06}N_{0.99})$ | 4.14735(8) | 36 |
| 0.2 | 1173 | 0.21 | 6.5(5) | 16.5(5) | $Cr_{0.8}Mo_{0.2}(O_{0.27}N_{0.93})$ | 4.15765(11) | 28 |
| 0.4 | 1173 | 0.43 | 1.7(1) | 14.5(4) | $Cr_{0.6}Mo_{0.4}(O_{0.09}N_{0.82})$ | 4.1688(3) | 18 |
| 0.5 | 1198 | 0.51 | 2.2(2) | 13.6(4) | $Cr_{0.5}Mo_{0.5}(O_{0.12}N_{0.85})$ | 4.1715(4) | 21 |
| 0.6 | 1173 | 0.61 | 1.1(1) | 12.3(4) | $Cr_{0.4}Mo_{0.6}(O_{0.06}N_{0.80})$ | 4.1783(3) | 21 |
| 0.8 | 1123 | 0.82 | 1.8(1) | 10.0(3) | $Cr_{0.2}Mo_{0.8}(O_{0.11}N_{0.78})$ | 4.1876(3) | 18 |
| 1.0 | 1073 | — | 3.8(3) | 8.4(3) | $Mo(O_{0.26}N_{0.66})$ | 4.1937(3) | 16 |

[a]Estimated absolute error in $z$ is 0.02.

work was to investigate the optimal conditions for obtaining the cubic phase containing Cr only with our experimental array when starting from freeze-dried precursors (it must be stressed that there is evidence for the formation of different molybdenum nitrides from ammonolysis processes, depending on both the procedural variables and the nature of the molybdenum source).[10,11]

Taking as reference our previous results, we carried out preliminary ammonolysis processes on the amorphous solid precursors containing Cr only. We used long reaction times (12 h, to eliminate time as a variable) and temperatures ranging from 873 to 1173 K. In this way, it was also possible to evaluate the influence of the cooling rate, another variable that is sometimes key in this type of process.[3] Fig. 1 shows X-ray diffraction patterns of the products resulting from the ammonolysis process when subjected to a fast cooling rate after treatment at the indicated temperature. As can be observed, the cubic phase (δ-CrN, JCPDS Card 11-0065) is obtained at temperatures between 1023 and 1173 K. On the other hand, as occurred for δ-VN, this result is independent of the cooling rate. Thus, concerning the systems we are dealing with, the cooling rate apparently only plays a significant role in the synthesis of the Mo-containing samples (quenching is required to obtain the cubic γ-$Mo_2N$ phase). In any case, given that we were looking to harmonize the synthetic parameters in all three individual nitride systems, we adopted quenching as a fixed condition in our preparative procedure.

From the above, we selected a nitridation temperature of 1073 K and fast cooling rates, after 2 h of thermal treatment, as the conditions to be adopted for the preparation of compounds in the $V_{1-z}Cr_z(O_xN_y)$ series. Under these conditions, all compositions ($0 \leqslant z \leqslant 1$) in this series are prepared as single phases. The significant shortening of the reaction time, with regard to our preliminary experiments, did not change the result; reaction times as short as 12 min also yield single phase products. However, when the same experimental procedure is applied for obtaining compounds in the $Cr_{1-z}Mo_z(O_xN_y)$ series, a certain amount of impurities are observed, together with the respective bimetallic oxynitride phases. The detected impurities are $Cr_2O_3$ and $MoO_3$ (JCPDS 38,1479 and 35,0609, respectively). At this point, our immediate goal was to explore procedural modifications to minimize the amount of impurities. With this aim, we again opted to use long reaction times (12 h) and carried out nitridation experiments at different temperatures for each composition in the $Cr_{1-z}Mo_z(O_xN_y)$ series. To date, our best results correspond to the nitridation temperatures listed in Table 2; however, we have not been able to completely eliminate oxide impurities for all compositions in $Cr_{1-z}Mo_z(O_xN_y)$ ($0 \leqslant z \leqslant 1$).

Fig. 2 and 3 show X-ray diffraction patterns corresponding to samples of different compositions in the series $V_{1-z}Cr_z(O_xN_y)$ and $Cr_{1-z}Mo_z(O_xN_y)$ ($0 \leqslant z \leqslant 1$) prepared by nitridation of the respective freeze-dried precursors under the above established conditions. The patterns are characteristic of a rock salt structure. Cell parameters were calculated by profile fitting of the patterns using the LeBail method, as implemented in the FULLPROF program (Tables 1 and 2). In the case of $Cr_{1-z}Mo_z(O_xN_y)$ samples, the regions in which peaks from reflections due to impurities appear have been excluded from the refinements. Fig. 4 shows the variation of the cell parameter

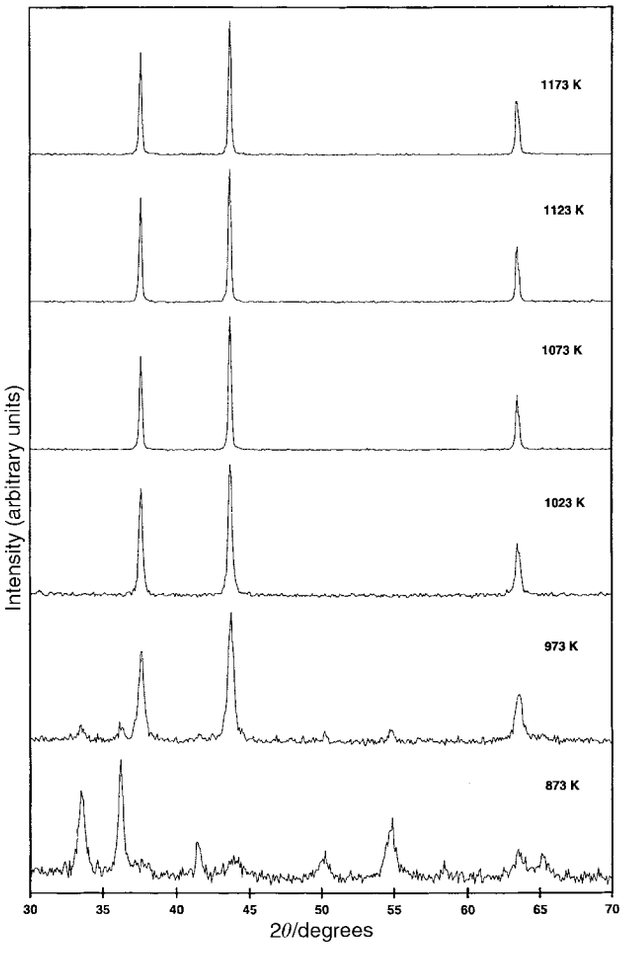


**Fig. 1** X-Ray diffraction patterns of the products resulting after ammonolysis of the freeze-dried precursor containing only chromium at different temperatures, after 12 h of thermal treatment and using fast cooling rates. The pattern at 873 K corresponds to $Cr_2O_3$ (JCDPS 38,1479); $Cr_2O_3$ is present as an impurity in the product obtained at 973 K.

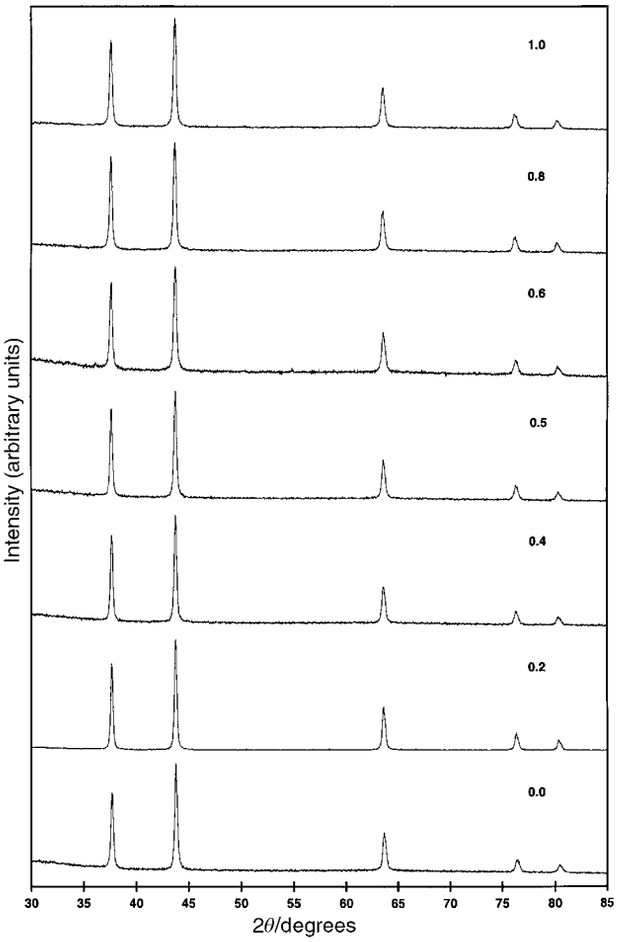


**Fig. 2** X-Ray diffraction patterns of $V_{1-z}Cr_z(O_xN_y)$ materials prepared by direct ammonolysis of freeze-dried precursors.

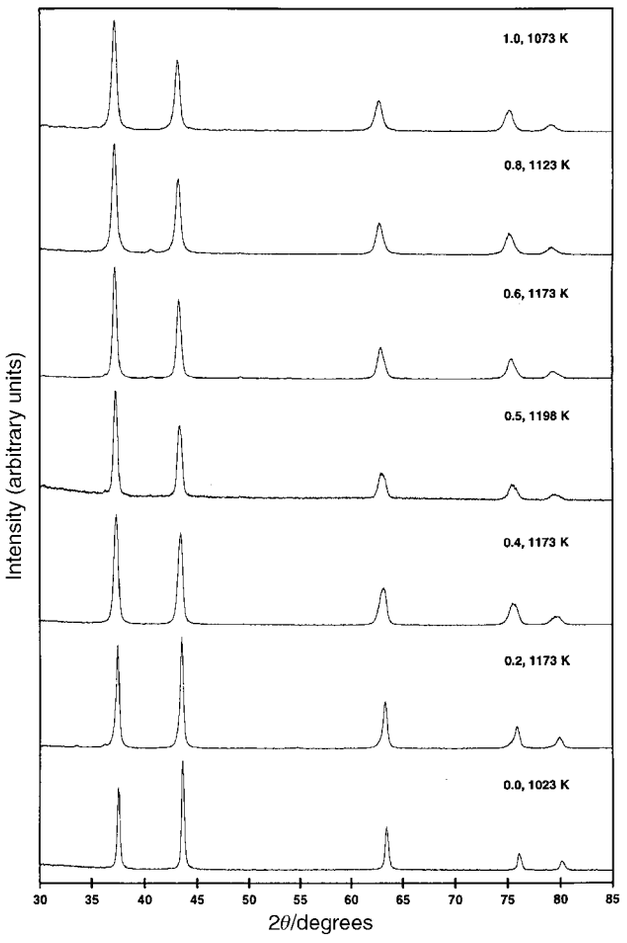


**Fig. 3** X-Ray diffraction patterns of $Cr_{1-z}Mo_z(O_xN_y)$ materials prepared by direct ammonolysis of freeze-dried precursors.

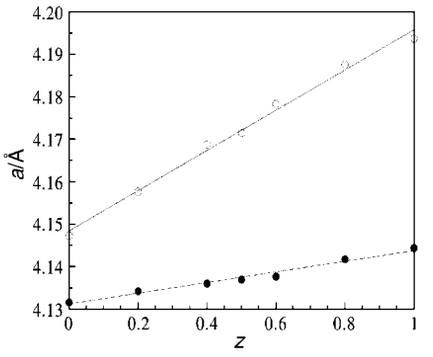


**Fig. 4** Cubic cell volume *versus* composition for $V_{1-z}Cr_z(O_xN_y)$ (●) and $Cr_{1-z}Mo_z(O_xN_y)$ (○). The solid lines correspond to the best linear fits to the data. Error bars are smaller than the points.

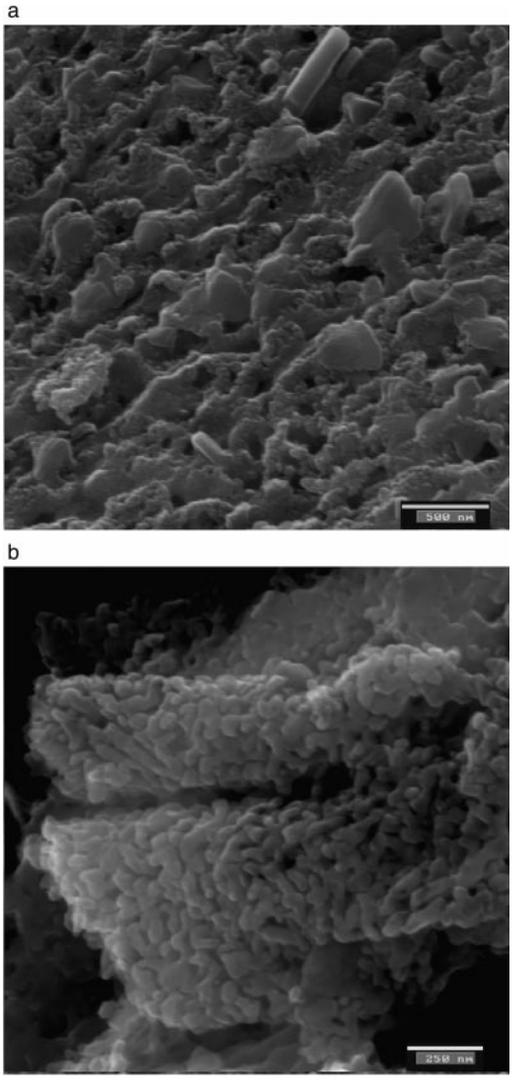


**Fig. 5** SEM images showing the microstructure of the precursor (a) and the oxynitride (b) in the $V_{1-z}Cr_z(O_xN_y)$ series. Scale bars correspond to 500 and 250 nm, respectively.

of the cubic structure with composition for $V_{1-z}Cr_z(O_xN_y)$ and $Cr_{1-z}Mo_z(O_xN_y)$. The cell dimensions of the synthesized oxynitrides fit well with those previously reported for related phases and for the individual nitrides δ-VN, δ-CrN and γ-$Mo_2N$.

Tables 1 and 2 show the results of chemical analysis of the resulting products (black powders). In all cases, the V : Cr and Cr : Mo ratios are (within experimental error) equal to the nominal value in the corresponding precursor. One aspect that deserves some explanation is the proposed nitrogen and oxygen stoichiometry. Previous work on $V_{1-z}Mo_z(O_xN_y)$ has shown that the oxygen content depends on the procedural variables.[1,3] Samples in the $V_{1-z}Cr_z(O_xN_y)$ and $Cr_{1-z}Mo_z(O_xN_y)$ solid solutions tend to be pyrophoric, which is why they must be passivated (treatment under $N_2$ atmosphere) prior to manipulation. The purpose of this passivation is to cover the active surface of the material with a layer of oxide ($O_2$ present as an impurity in $N_2$) to prevent oxidation of the bulk. Besides the incorporation of oxygen atoms in interstitial positions, surface oxidation is the main reason for the variable oxygen content in the solid.

Fig. 5 shows characteristic SEM images corresponding to representative samples in the $V_{1-z}Cr_z(O_xN_y)$ and $Cr_{1-z}Mo_z(O_xN_y)$ series. The freeze-dried precursor is comprised of very large sheets with a typical width of 2–5 μm. In turn, these large sheets consist of fine sheets with typical dimensions $300 \times 300 \times 30$ nm (Fig. 5a). The external appearance of the large sheets remains practically unchanged during the ammonolysis process yielding $V_{1-z}Cr_z(O_xN_y)$ and $Cr_{1-z}Mo_z(O_xN_y)$, but the fine structure is lost and the resulting large sheets show wrinkled surfaces. In fact, SEM images at high magnification clearly reveal that $V_{1-z}Cr_z(O_xN_y)$ and $Cr_{1-z}Mo_z(O_xN_y)$ grains are aggregates of nanometric spherical particles with typical diameters around 20 nm (Fig. 5b).

The size of the crystallites (Tables 1 and 2) has been calculated from XRD patterns by a standard Scherrer analysis of the half-width of the XRD peaks, using the (200) reflection. Well crystallized $Pb(NO_3)_2$ was used as standard to calibrate the intrinsic width associated with the equipment. Crystallite size remains practically constant (*ca.* 36 nm) along the

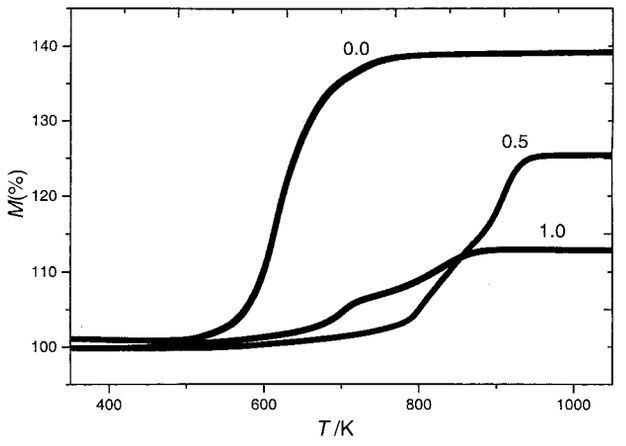


**Fig. 6** Characteristic TGA profiles corresponding to $V(O_xN_y)$ ($z=0$), $V_{0.5}Cr_{0.5}(O_xN_y)$ ($z=0.5$) and $Cr(O_xN_y)$ ($z=1$).

$V_{1-z}Cr_z(O_xN_y)$ series, whereas it decreases with $z$ along the $Cr_{1-z}Mo_z(O_xN_y)$ series (from 36 to 16 nm).

Fig. 6 shows characteristic TGA profiles for the single metal oxynitrides ($z=0$ and 1) and an intermediate composition ($z=0.5$) for the $V_{1-z}Cr_z(O_xN_y)$ series. The oxidation begins in all cases at relatively low temperatures (*ca.* 530–600 K) and is complete between 800 and 1030 K, depending on the composition. The final products are $V_2O_5$ (JCPDS 41,1426), for $z=0$, $Cr_2O_3$ (JCPDS 38,1479), for $z=1$, and $VCrO_4$ (JCPDS 38,1376), for $z=0.5$. For all the remaining intermediate compositions, a mixture of $VCrO_4$ and the respective single metal oxide (depending on the $z$ value) is obtained. In the $Cr_{1-z}Mo_z(O_xN_y)$ series, the oxidation begins also at relatively low temperatures (*ca.* 500–600 K) and is complete between 700 and 1050 K, depending on the composition. The final products are $Cr_2O_3$ (JCPDS 38,1479) for $z=0$, $MoO_3$ (JCPDS 35,0609) for $z=1$, and $CrMoO_4$ (JCPDS 29,0452) for $z=0.5$. For all the remaining intermediate compositions, a mixture of $CrMoO_4$ and the respective single metal oxide (depending on the $z$ value) is obtained. Low temperature oxidation is consistent with the pyrophoric character of these products, which makes passivation necessary. Surface oxidation must account to a great extent for the oxygen content of these oxynitrides.

## Concluding remarks

By preparing the rock salt-type phases in the solid solutions series $V_{1-z}Cr_z(O_xN_y)$ and $Cr_{1-z}Mo_z(O_xN_y)$ ($0\leqslant z\leqslant 1$) in the first place we are verifying the versatility of a relatively simple processing route to complex *ad hoc* compositions. On the other hand, at the expense of some minor procedural refinements, the objective of obtaining any composition with the rock salt structure in the trimetallic V–Cr–Mo–O–N system seems reasonably accessible. It should then be possible to explore the catalytic properties of this system depending not only on the stoichiometric metal ratio as a whole, but also on the subtle chemical differences which arise from metal substitutions. In fact, insofar as they affect the sensitivity of the resulting material towards oxidation (redox behaviour), there are very likely to be metal substitutions which account for the above-mentioned problems associated with the preparation of Mo-containing samples. Beyond the synthetic problem, learning to modulate the redox behaviour of the material should be relevant to improvement of the catalytic performance in processes involving hydrogen transfer reactions.

## Acknowledgements

This research was supported by the Spanish Comisión Interministerial de Ciencia y Tecnología (MAT96-1037, PB98-1424). The SCSIE of the Universitat de València is acknowledged for X-ray diffraction, microscopy and analytical facilities.

## References

1 A. El-Himri, M. Cairols, S. Alconchel, F. Sapiña, R. Ibañez, D. Beltrán and A. Beltrán, *J. Mater. Chem.*, 1999, **9**, 3167.
2 *The Chemistry of Transition Metal Carbides and Nitrides*, ed. S. T. Oyama, Blackie Academic & Professional, Chapman & Hall, London, 1996, p. 1; *International Symposium on Nitrides*, in *J. Eur. Ceram. Soc.*, ed. Y. Laurent and P. Verdier, 1997, vol. 17, pp. 1773–2037; D. H. Gregory, *J. Chem. Soc., Dalton Trans.*, 1999, 259; R. Niewa and F. J. DiSalvo, *Chem. Mater.*, 1998, **10**, 2733.
3 C. C. Yu, S. Ramanathan, F. Sherif and S. T. Oyama, *J. Phys. Chem.*, 1994, **98**, 13038; C. C. Yu and S. T. Oyama, *J. Solid State Chem.*, 1995, **116**, 205; C. C. Yu and S. T. Oyama, *J. Mater. Sci.*, 1995, **30**, 4037; R. Kapoor, S. T. Oyama, B. Frühberger and J. G. Chen, *J. Phys. Chem. B*, 1997, **101**, 1543; C. C. Yu, S. Ramanathan and S. T. Oyama, *J. Catal.*, 1998, **173**, 1; S. Ramanathan, C. C. Yu and S. T. Oyama, *J. Catal.*, 1998, **173**, 10; S. T. Oyama, C. C. Yu and F. G. Sherif, *US Patent* 5 444 173, 1995.
4 S. Alconchel, F. Sapiña, D. Beltrán and A. Beltrán, *J. Mater. Chem.*, 1999, **9**, 749.
5 S. Alconchel, F. Sapiña, D. Beltrán and A. Beltrán, *J. Mater. Chem.*, 1998, **8**, 1901.
6 A. Le Bail, H. Duroy and J. L. Fourquet, *Mater. Res. Bull.*, 1988, **23**, 447.
7 J. Rodriguez-Carvajal, FULLPROF Program, personal communication.
8 V. Primo, *Powder Diffr.*, 1999, **14**, 70.
9 P. Ettmayer and W. Lengauer, in *Encyclopedia of Inorganic Chemistry*, ed. R. Bruce King, John Wiley and Sons, Chichester, 1994, p. 2498.
10 C. H. Jaggers, J. N. Michaels and A. M. Stacy, *Chem. Mater.*, 1990, **2**, 150.
11 R. Marchand, F. Tessier and F. J. DiSalvo, *J. Mater. Chem.*, 1999, **9**, 297.